

Satellite Radiance Data Assimilation within the Hourly Updated Rapid Refresh

HAI DAO LIN,^a STEPHEN S. WEYGANDT, STANLEY G. BENJAMIN, AND MING HU^b

NOAA/OAR/Earth System Research Laboratory, Boulder, Colorado

(Manuscript received 6 December 2016, in final form 4 April 2017)

ABSTRACT

Assimilation of satellite radiance data in limited-area, rapidly updating weather model/assimilation systems poses unique challenges compared to those for global model systems. Principal among these is the severe data restriction posed by the short data cutoff time. Also, the limited extent of the model domain reduces the spatial extent of satellite data coverage and the lower model top of regional models reduces the spectral usage of radiance data especially for infrared data. These three factors impact the quality of the feedback to the bias correction procedures, making the procedures potentially less effective. Within the National Oceanic and Atmospheric Administration (NOAA) Rapid Refresh (RAP) hourly updating prediction system, satellite radiance data are assimilated using the standard procedures within the Grid-point Statistical Interpolation (GSI) analysis package. Experiments for optimizing the operational implementation of radiance data into RAP and for improving benefits of radiance data have been performed. The radiance data impact for short-range forecasts has been documented to be consistent and statistically significantly positive in systematic RAP retrospective runs using real-time datasets. The radiance data impact has also been compared with conventional observation datasets within RAP. The configuration for RAP satellite radiance assimilation evaluated here is that implemented at the National Centers for Environmental Prediction (NCEP) in August 2016.

1. Introduction

The Rapid Refresh (RAP; Benjamin et al. 2016, hereafter B16) is a National Oceanic and Atmospheric Administration (NOAA) operational mesoscale hourly updated assimilation/prediction model run at the National Centers for Environmental Prediction (NCEP). Because of the increased domain coverage of RAP (Fig. 1 in B16) compared with its predecessor, the Rapid Update Cycle (RUC; Benjamin et al. 2004a), satellite radiance data now play a role in hourly model assimilation and forecast skill. The incorporation of satellite radiance data into RAP is

one of the noticeable differences between the RAP and RUC. Our related study (Lin et al. 2017, manuscript submitted to *Wea. Forecasting*) shows that the Atmospheric Infrared Sounder (AIRS; Aumann et al. 2003) data have a small positive impact within a 3-h cycled older RAP version using full radiance coverage datasets (no limits on data usage because of real-time data cutoff issues) for research purposes. Here, we look at the impact of real-time satellite radiance data for short-range forecasts (0–18 h) and how to maximize the data impact within the real-time high-frequency updated regional models.

Satellite radiance data have been directly assimilated effectively through the use of radiative transfer models and variational assimilation schemes in virtually all operational numerical weather prediction (NWP) centers (Andersson et al. 1994; Derber and Wu 1998; McNally et al. 2000, McNally et al. 2006) and have become the most important observation datasets for global models. Procedures for the direct assimilation of radiance data into global models are well established, and the significant positive impact of radiance data within global models has been well demonstrated (e.g., Jung et al. 2008; McNally 2012; Lord et al. 2016; Boukabara et al. 2016).

 Denotes content that is immediately available upon publication as open access.

^a Additional affiliation: Cooperative Institute for Research in the Atmosphere, Colorado State University, Fort Collins, Colorado.

^b Additional affiliation: Cooperative Institute for Research in Environmental Sciences, University of Colorado Boulder, Boulder, Colorado.

Corresponding author: Haidao Lin, haidao.lin@noaa.gov

DOI: 10.1175/WAF-D-16-0215.1

© 2017 American Meteorological Society. For information regarding reuse of this content and general copyright information, consult the [AMS Copyright Policy](#) (www.ametsoc.org/PUBSReuseLicenses).

The direct assimilation of radiance data into regional models, however, still remains a challenge as a result of nonuniform and limited data coverage, radiance bias correction, and relatively lower model tops compared with global models. Some NWP centers are currently exploring the maximum impact of radiance data into regional models by overcoming the difficulties inherent in the regional radiance assimilation (e.g., [Kazumori 2014](#)). By reducing the amount of data thinning, extrapolating the atmospheric profiles from mesoscale model top to the radiative transfer model top, and using the bias correction coefficients estimated from global models, [Kazumori \(2014\)](#) showed improvements in regional-model forecasts of troposphere geopotential height and precipitation, using mostly microwave and imager data.

Maximizing data coverage becomes a more difficult challenge for high-frequency updating regional systems. The very short observation cutoff time (~ 35 min) and the long data latency, especially for polar-orbiter satellites, pose significant challenges for maximizing real-time data coverage. The reduction of data latency is crucial for rapidly updating model systems. Sparse data coverage associated with limited domain size and a lower model top with fewer levels in the stratosphere compared with most global models further reduces the effectiveness of the regional radiance bias correction. The lower model top and fewer atmospheric layers can result in radiance data that have less utility. Noting these challenges, we evaluate the impact from satellite radiance data on the real-time operational RAP and develop a design to improve the benefits from these data. Here, we developed a series of radiance updates and tested their effectiveness for better radiance assimilation within RAP. These radiance updates included using the Regional ATOVS Retransmission Services [RARS; short latency direct readout; [WMO \(2009\)](#)] direct-readout data to reduce the real-time data latency, channel selection to remove the high peaking channels (also ozone channels) to reduce the adverse impact from the relatively low model top, and the usage of enhanced variational bias correction with cycling developed by NCEP ([Zhu et al. 2014](#)) to obtain a more robust, efficient, and stable radiance bias-correction procedure. These settings/updates for improved satellite radiance assimilation with an hourly model were implemented in RAP version 3 (RAPv3) at NCEP during August 2016. This study is the first to give an overall evaluation and impact assessment of real-time satellite radiance data on short-range forecasts within the RAP.

A series of 1-month retrospective experiments has been performed with and without the real-time

radiance data (also with and without the direct-readout data) to evaluate the radiance data impact using RAP version 3. RAPv3 covers a greater proportion of oceanic areas than do RAPv1 and RAPv2 (Fig. 1 in [B16](#)), with yet more need for effective satellite radiance assimilation. Furthermore, because satellite radiances are a principal new dataset in RAP compared with the RUC, the impact of radiance data is also compared with other conventional datasets (aircraft and radiosonde data) to quantify the relative magnitude of the impact from the radiance data within RAP through several 1-month data-denial retrospective runs. This paper complements the RAP observation impact experiments for non-radiance observations described by [James and Benjamin \(2017\)](#).

The paper is organized as follows: a brief description of the RAP model system is given in [section 2](#). [Section 3](#) gives the overall radiance updates/settings for RAP version 3 including the discussion of real-time satellite radiance coverage and the usage of the RARS direct-readout data in RAP, the channel selection process designed to fit RAP's model top, and the implementation and assessment of the enhanced variational bias correction with cycling in RAP. [Section 4](#) provides the experiment design, results, and discussion about the radiance data impact in RAP as well as the relative radiance data impact comparison with conventional datasets from several 1-month retrospective runs. [Section 5](#) provides conclusions and outlines our future work.

2. Rapid Refresh model system

The RAP mesoscale assimilation and forecast system was developed by the Global Systems Division (GSD) of the NOAA's Earth System Research Laboratory (ESRL) in collaboration with other laboratories and has run operationally at NCEP since 2012. The RAP configuration as it is being used operationally at NCEP in 2016 is described in [B16](#). The version of the RAP used in this study employed the code developed at ESRL/GSD as of mid-2015, a development version toward RAP version 3 (operationally implemented at NCEP in August 2016), which included the advanced GSI hybrid variational-ensemble Kalman filter (EnKF) data assimilation system and the full radiance updates for RAP version 3.

The RAP model utilizes Gridpoint Statistical Interpolation (GSI; [Wu et al. 2002](#); [Kleist et al. 2009](#)) for the analysis component and the Advanced Research version of the Weather Research and Forecasting Model (WRF-ARW; [Skamarock et al. 2008](#)) for the

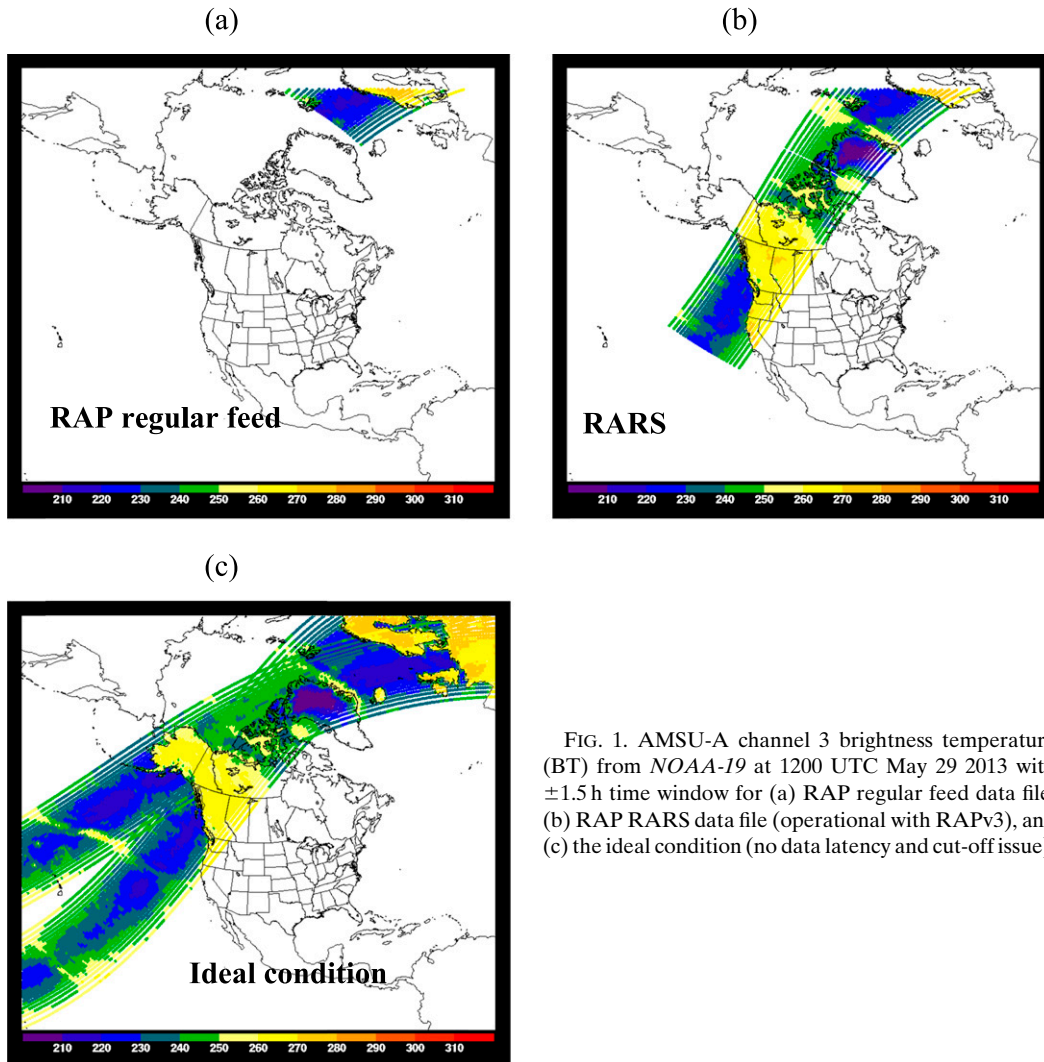


FIG. 1. AMSU-A channel 3 brightness temperature (BT) from *NOAA-19* at 1200 UTC May 29 2013 with ± 1.5 h time window for (a) RAP regular feed data file, (b) RAP RARS data file (operational with RAPv3), and (c) the ideal condition (no data latency and cut-off issue).

forecast component. WRF version 3.6 is used in this study. Beginning with RAP version 2 (operationally implemented at NCEP during February 2014), the advanced GSI hybrid EnKF data assimilation system was implemented using ensemble information from the NCEP 80-member global ensemble data assimilation system.

RAP operates at 13-km horizontal resolution (see Fig. 1 in B16 for the RAPv3 domain), with 954×835 grid points and 50 vertical computational layers, and a 10-hPa model top. In addition to conventional data, satellite radiance data are also assimilated in the RAP through the Community Radiative Transfer Model (CRTM; Han et al. 2006; Weng 2007) built within GSI. Only clear-sky radiance data are assimilated in the version of GSI employed for the RAP. Forecasts from the NCEP Global Forecast System (GFS) are introduced twice daily into RAP through two partial

cycles (0300–0800 and 1500–2000 UTC), as described in B16. In contrast to the full cycles (24 cycles from 0000 to 2300 UTC each day), which have longer (up to 18 h for NWP guidance) forecasts, each partial cycle has a 1-h forecast for the purpose of advancing the cycle. The GFS also provides lateral boundary conditions for the RAP forecasts. Surface fields (e.g., snow cover, soil moisture) are continuously hourly cycled within the RAP independent of the GFS.

3. Radiance assimilation for RAP version 3

a. Real-time radiance data coverage

Consistent with the short-range “situational awareness” niche that RAP and the High Resolution Rapid Refresh (HRRR; Smith et al. 2008, B16) occupies within the NCEP suite of models and with its

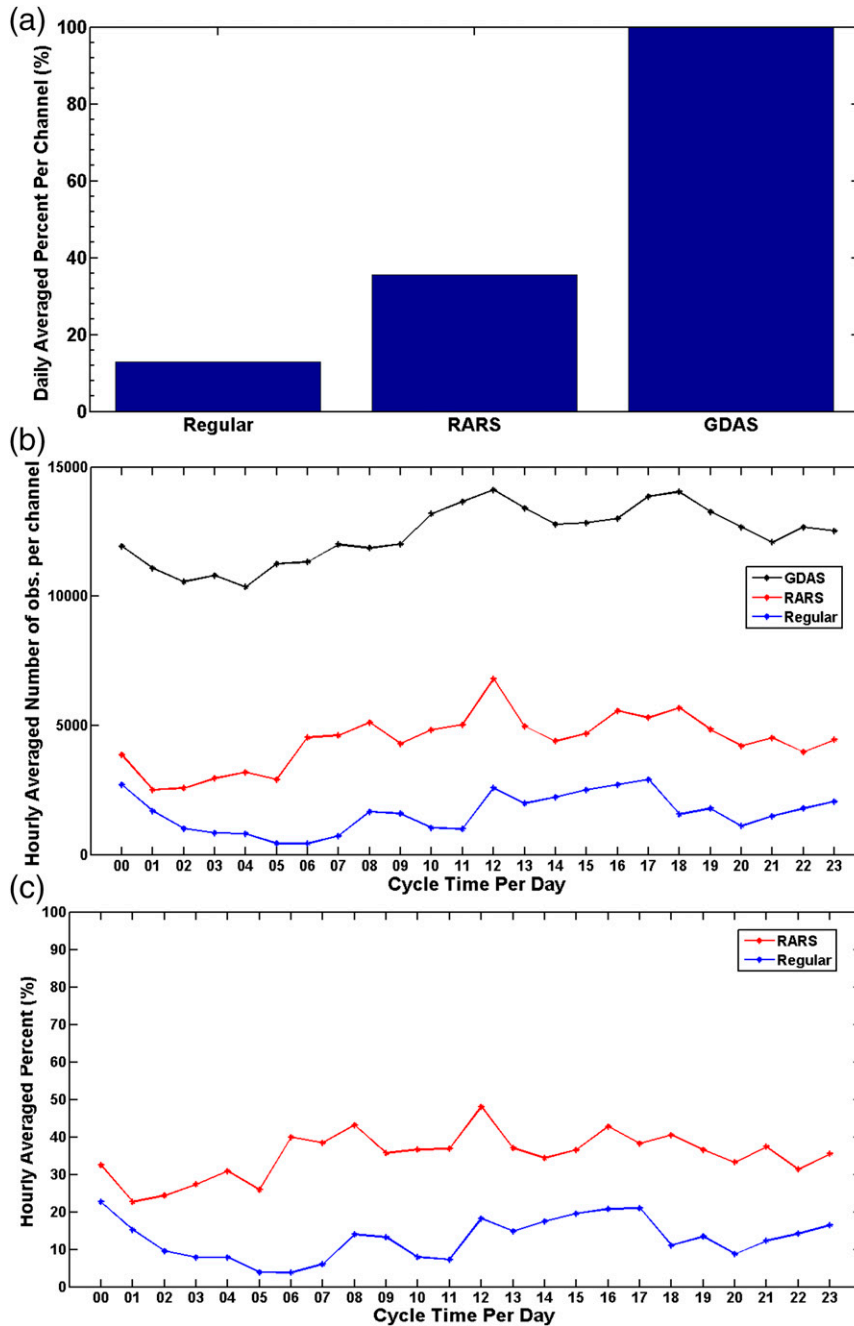


FIG. 2. (a) Daily averaged percent (%) and (b) hourly averaged observation number for regular feed, RARS feed, and ideal GDAS conditions and (c) hourly averaged observation percent for regular feed and RARS feed against ideal conditions. Statistics are computed from NOAA-19 AMSU-A channel 3 over the RAP domain over a 1-month period (1–31 May 2013). The time window is ± 1.5 h.

hourly updated cycling frequency, RAP and HRRR use a short observation data cutoff time of about +35 min after the analysis time. For satellite data, this short observation cutoff time poses significant challenges. With the hourly cycling nature of the regional

RAP model, the maximum areal extent of polar-orbiting satellite data coverage for a given hour is already limited because of the short data-use window. For RAP, this window extends back no more than 1.5 h from the model initial time. This already limited

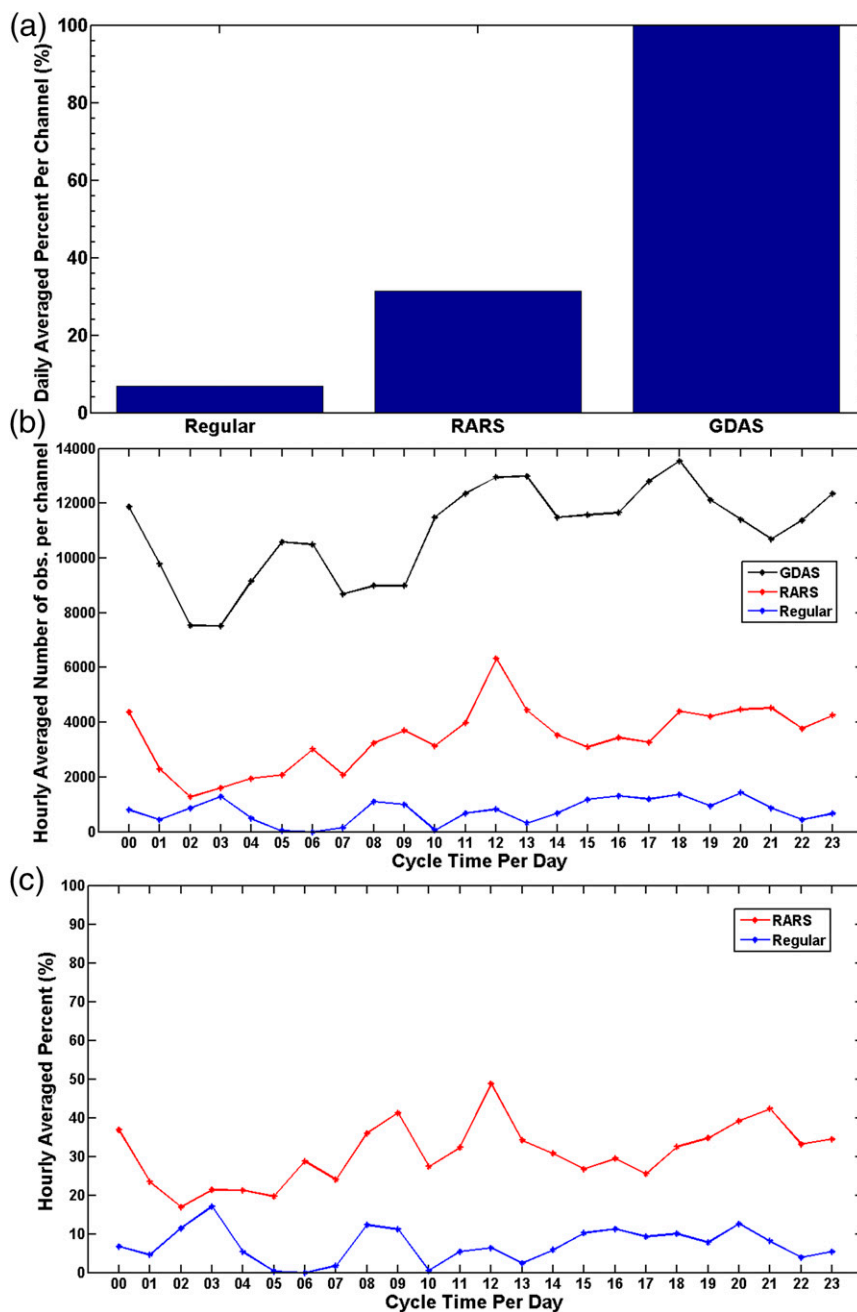


FIG. 3. As in Fig. 2 but for the NOAA-18 satellite platform.

areal coverage is further reduced when increased data latency delays the time of the data availability. This can lead to a situation where most (or even all) of the observation data that are available by the observation cutoff time are too old to be used (observations are available before the beginning of the data-use window). This issue significantly limits the utility of satellite data in high-frequency assimilation systems such as RAP.

To provide some illustration of this satellite latency issue for RAP (which also affects HRRR since RAP is used to initialize HRRR), spot-check evaluations for some RAP regular real-time satellite data files and the RARS files for RAP were completed. The RARS project aims to provide real-time satellite data for NWP models with reduced data latency via locally received direct-readout reception systems (WMO 2009). Figure 1 shows the NOAA-19 AMSU-A data coverage at 1200 UTC

TABLE 1. List of AMSU-A, MHS, HIRS-4, and GOES sounder channels used in the retrospective runs.

Satellite	Sensor	Channels assimilated
<i>NOAA-15</i>	AMSU-A	1–10 and 15
<i>NOAA-18</i>	AMSU-A	1–8, 10, and 15
	MHS	1–5
<i>NOAA-19</i>	AMSU-A	1–7, 9–10, and 15
	MHS	1–5
<i>MetOp-A</i>	AMSU-A	1–6, 8–10 ^a , and 15
	MHS	1–5
	HIRS-4	4–8 and 10–15
<i>MetOp-B</i>	AMSU-A	1–10 and 15
<i>GOES-15</i>	MHS	1–5
	Sounders (s ndrD1, s ndrD2, s ndrD3, and s ndrD4)	3–8 and 10–15

^a As of 26 September 2014, channel 8 from *MetOp-A* was removed from operational RAP per an NCEP note indicating channel 8 had gone bad.

29 May 2013 for the RAP real-time regular feed (RAPv2 feed) data file, a RARS data file for RAP, and the ideal conditions [no data latency or data cutoff issues, data from NCEP's Global Data Assimilation System (GDAS)]. As Fig. 1 shows, for this cycle time, just a small amount of data was available in the data-use window in

the RAP real-time file (Fig. 1a). In contrast, data coverage from the RARS file (Fig. 1b) is better, due to the lower latency from the direct readout. Figure 1c shows the coverage for no latency, the best possible condition. To obtain a more complete picture of the real-time radiance data availability, we have examined the real-time RAP radiance data for a 1-month (May 2013) period. Figures 2 and 3 show the statistical results based on 1-month datasets for AMSU-A channel 3 from the *NOAA-19* platform and the *NOAA-18* platform, respectively. It can be seen that the data from the operational RAPv2 feed have a daily average of 13% for *NOAA-19* and 6.9% for *NOAA-18* availability whereas the RARS feed provides around 36% availability for *NOAA-19* and 31% for *NOAA-18*, thus showing that the RARS feed data can increase the hourly radiance data coverage for RAP. The results are similar regardless of time of day (Figs. 2b,c and 3b,c). Although the RARS feed dataset significantly increases the daily coverage, it is still short of full data usage. As these examples illustrate, satellite data latency issues significantly limit the utility of these data for high-frequency data assimilation systems but access to low-rate data (LRD) via direct readout is critical for improved data coverage in

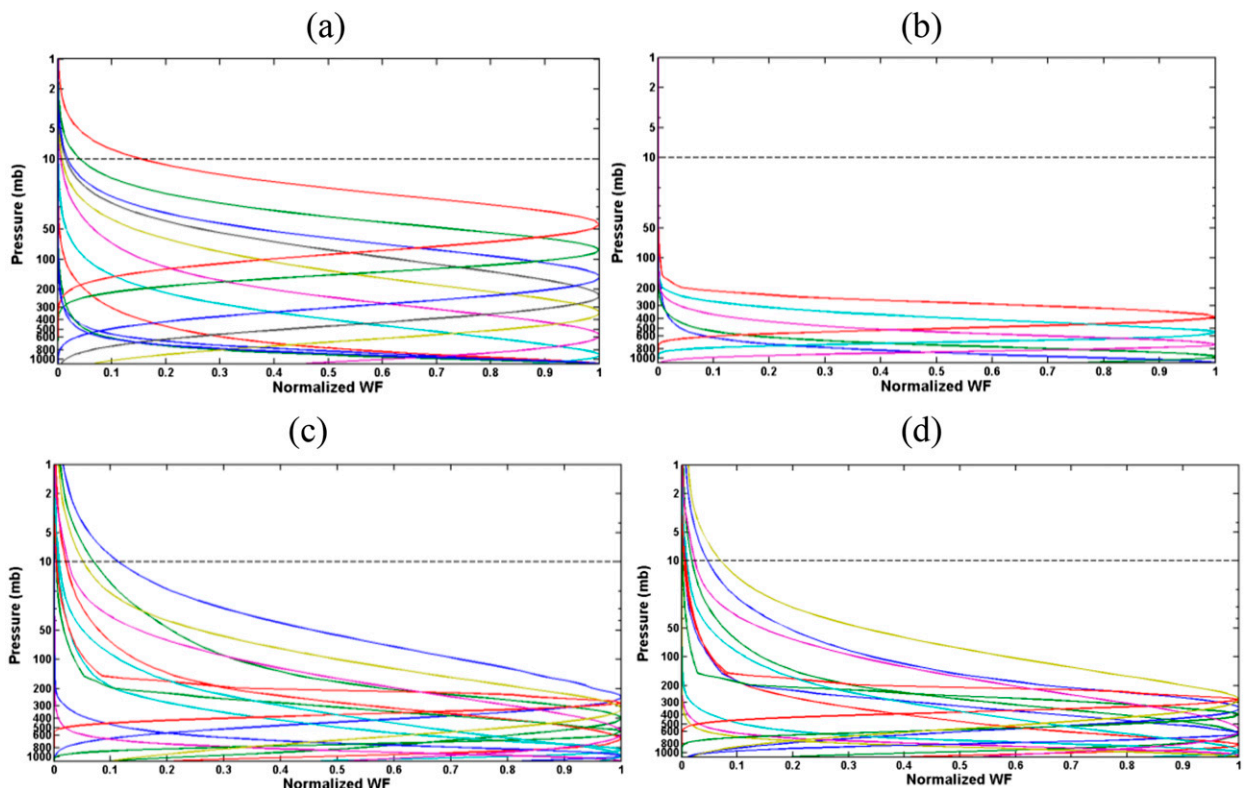


FIG. 4. Normalized weighting function of used channels in RAP for (a) AMSU-A onboard *NOAA-15*, (b) MHS onboard *NOAA-18*, (c) HIRS-4 onboard *MetOp-A*, and (d) GOES sounder (s ndrD1) onboard *GOES-15*. The dashed line indicates the RAP 10-hPa model top.

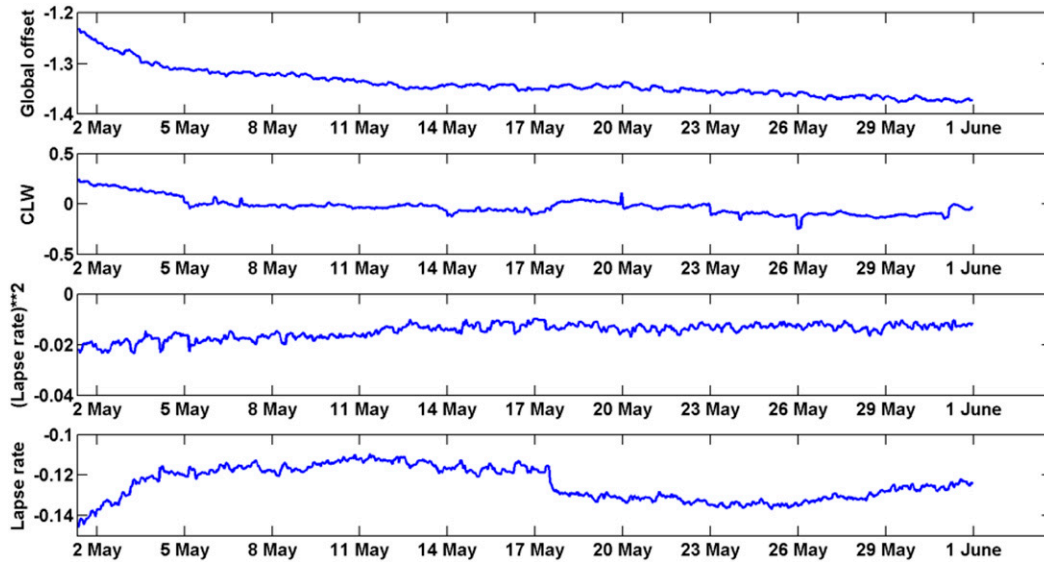


FIG. 5. Time series of the coefficients of air-mass bias correction predictors (global offset, cloud liquid water, square of lapse rate, and lapse rate) for *NOAA-18* AMSU-A channel 6 from the 1-month (1–31 May 2013) control experiment using RAP.

RAP. Accordingly, the RARS feed dataset has been adopted for use in RAP version 3, partially as an outcome of this study.

b. Channel selection

As the RAP system has a low model top of 10 hPa, satellite channels with a peak weighting function (PWF) above or near the RAP model top are not assimilated. For a specific channel, if the transmittance calculated from CRTM from the model top to the top

of atmosphere (TOA) is more than 10% of the total transmittance contribution, then this channel is removed. Channel selection for RAP [AMSU-A, Microwave Humidity Sounder (MHS), HIRS-4, and GOES sounder] has been performed, removing the high-level and ozone channels. The channels selected for RAP are listed in Table 1. These channels are currently used in the operational version of RAP (RAPv3) at NCEP. Figure 4 shows the weighting functions of the channels used in RAP for four satellite platforms (AMSU-A on

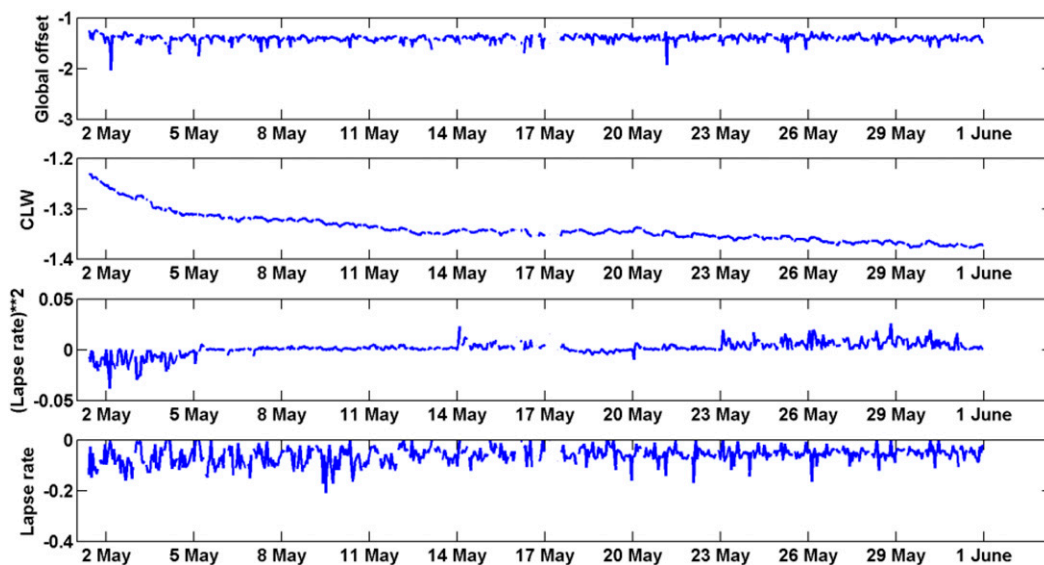


FIG. 6. As in Fig. 5, but for time series of the mean (cycle averaged) bias correction terms (K).

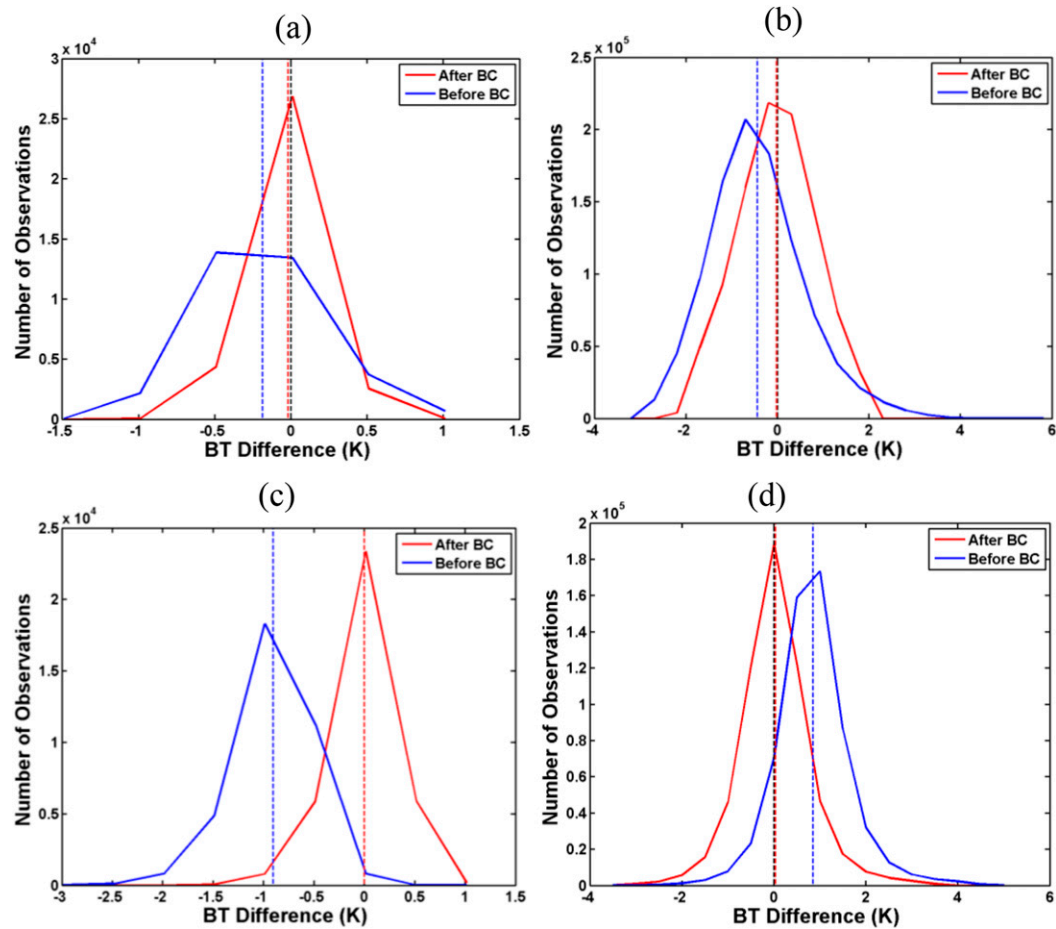


FIG. 7. Histogram of BT $O - B$ values before (blue) and after BC (red) for (a) AMSU-A channel 5 on *NOAA-15*, (b) MHS channel 5 on *NOAA-18*, (c) HIRS-4 channel 6 on *MetOp-A*, and (d) GOES sounder (s ndrD1) channel 11 on *GOES-15*. Statistics obtained from the 1-month control run (including all observations). The dashed blue line indicates the mean value for the blue line, and the dashed red line indicates the mean value for the red line. The thick dashed black line is the zero line.

NOAA-15, MHS on *NOAA-18*, HIRS-4 on *MetOp-A*, and the GOES sounder on *GOES-15*). It can be seen that the channels with peak weighting functions as high as ~ 50 hPa are usable in RAP.

c. Bias correction

Bias correction is needed because satellite radiance data have biases due to calibration errors, the accuracy of the radiative transfer models, and systematic errors in the NWP short-term forecasts. GSI uses a variant of the variational radiance bias-correction scheme (Derber and Wu 1998; Dee 2005; Zhu et al. 2014). RAP version 3 uses the GSI enhanced radiance bias-correction (BC) scheme (Zhu et al. 2014) with the one-step airmass and scan-angle components both updated inside GSI. The airmass component is a linear combination of a set of predictors. There are four predictors in the enhanced radiance bias correction: global offset, cloud liquid water (for microwave

data), temperature lapse rate, and the square of the temperature lapse rate. The scan-angle bias correction term is expressed as a third- or fourth-order polynomial of the scan angle. All airmass and scan-angle bias coefficients are updated together with analysis control variables inside the GSI minimization process (Zhu et al. 2014). The airmass and angle bias coefficients are cycled hourly inside RAP. To further illustrate the time evolution of the airmass bias correction, Figs. 5 and 6 show the 1-month time evolution of the airmass bias coefficients (Fig. 5) and the cycle-averaged airmass bias correction terms (Fig. 6) for *NOAA-18* AMSU-A channel 6 from a RAP retrospective experiment (1–31 May 2013) that assimilates all the radiance data considered in this paper (summarized in Table 1). This experiment, which also includes all the conventional observations, will serve as the control experiment and will be further described in section 4a. Figure 7 shows

TABLE 2. Types of data used in the CNTL experiment.

Observation	Platform
Conventional	
Upper air	Sonde, profiler, and aircraft
Land surface	METAR and mesonet
Marine surface	Ship and buoys
Radar	VAD winds
Satellite	
Satellite winds (AMV)	GOES
Precipitable water	GPS
Microwave radiances	AMSU-A and MHS
Infrared radiances	HIRS-4 and GOES sounder

the histograms of observation minus background ($O - B$) values after (red) and before (blue) BC was applied for several representative channels from the AMSU-A, MHS, HIRS-4, and *GOES-15* sounder datasets. Statistics are based on the same 1-month control run. After BC, the mean values of $O - B$ are closer to zero for these channels compared with those before BC. This demonstrates that the BC procedure is functioning properly.

4. Experiment design and results

a. Retrospective experiments

To evaluate the impact of real-time radiance data within RAP, 5-month-long (1–31 May 2013) retrospective RAP hourly runs were completed: a control run (CNTL) and four data-denial runs. These runs were started at 0300 UTC 1 May 2013. An 18-h forecast is produced at each full cycle. The control run assimilated all operational real-time conventional and satellite radiance datasets as used in RAP version 3. All available conventional data, which include radiosondes, NOAA profilers, velocity–azimuth displays (VADs) winds, aviation routine weather reports (METARs; surface), buoys/ships, mesonets, global positioning system (GPS) derived precipitable water results, and satellite-derived atmospheric motion vector (AMV) winds, were assimilated in the CNTL run (see Table 2). Satellite radiance data included in the CNTL run were data from the AMSU-A, MHS, and HIRS-4 (low spectral infrared data). RARS data are used for radiance transmission

for these RAP experiments. In this study, the RARS data are applicable to AMSU-A and MHS data on the *NOAA-18*, *NOAA-19*, *MetOp-A*, and *MetOp-B* satellite platforms. A complete list of data assimilated in the CNTL run is given in Table 2. Four data-denial experiments were performed, including RARS, all-radiance, aircraft, and radiosonde denial. Table 3 shows the list of these five retrospective runs with observation types withheld. The RARS data-denial experiment (removing the RARS direct-readout radiance data only, all other data retained as with CNTL) is used to evaluate the added impact from the real-time RARS data as well as to preevaluate the benefits from future direct-readout data. The all-radiance data-denial run (removal of all radiance data including RARS data) is used to evaluate the overall impact from the radiance data within RAP. This will also show the impact from radiance data within the operational RAP (RAPv3). To show the relative impact of radiance data to other observations, two more data-denial runs were conducted: one for aircraft (including temperature, wind, and relative humidity) and one for radiosondes (including temperature, relative humidity, wind, and surface pressure). All four of the data-denial experiments will be compared with the CNTL results through the radiosonde verification for temperature, relative humidity, and wind.

A thinning mesh of 60 km was used for all radiance data in this study as the scale at which radiance observation errors are assumed to be uncorrelated. The observation errors used for all radiance channels assimilated in this study were obtained from the NCEP GDAS.

b. Results

We evaluated the data impact through the comparison of all four data-denial experiments with the CNTL run as verified against the available rawinsonde data in the RAP domain over a 1-month period. The rawinsonde verification procedure used in this study follows Benjamin et al. (2004a), Benjamin et al. (2010), and Moninger et al. (2010). In these data-denial experiments (Table 3), we compare forecast results of the CNTL run when all data are used against

TABLE 3. Observation impact experiments in this study. Those observational variables denied in RAP are shown for each experiment: radiance, temperature T , horizontal wind V , relative humidity (RH), and surface pressure (Ps).

Expt	Observation type and variable denied
CNTL: all observations used	
No RARS radiance	Radiance BT (AMSU-A, MHS) from RARS direct readout data
No radiance	Radiance BT (AMSU-A, MHS, HIRS-4, GOES sounder), including RARS data
No aircraft	Aircraft V , T , RH
No radiosonde	Rawinsonde T , V , RH, Ps

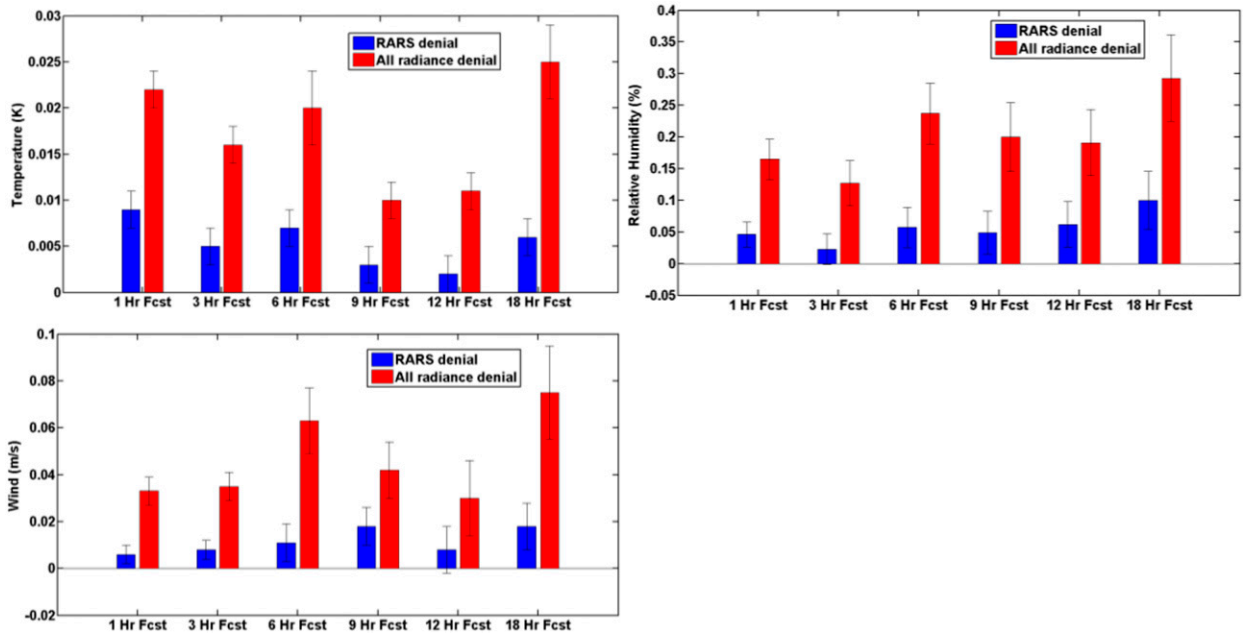


FIG. 8. RMSE reduction (EXPT – CNTL) for (top left) temperature (K), (top right) relative humidity (%), and (bottom left) vector wind magnitude ($m s^{-1}$) from the RARS denial run (blue) and all-radiance denial run (red) 1–18 h forecasts against rawinsonde observations. Statistics are computed for 1000–100-hPa layer over the RAP domain. The retrospective period is 1–31 May 2013. The error bar indicates the ± 1.96 standard error from the mean impact, representing the 95% confidence threshold for significance.

the selective denial of certain data classes as noted in Table 3. A positive impact of a data source thus indicates that the CNTL, with that data type present, produced better forecasts than the experiment in which that data type was not used. The metric for the quantitative impact of a data source is normalized reduction in root-mean-square

error (RMSE) [i.e., $(EXPT - CNTL)/CNTL$, more details about the normalized percentage impact can be found in Benjamin et al. (2004b)], where EXPT is the RMSE of the experiment in which the given data type is not used and CNTL is the RMSE of the control experiment in which all data are used.

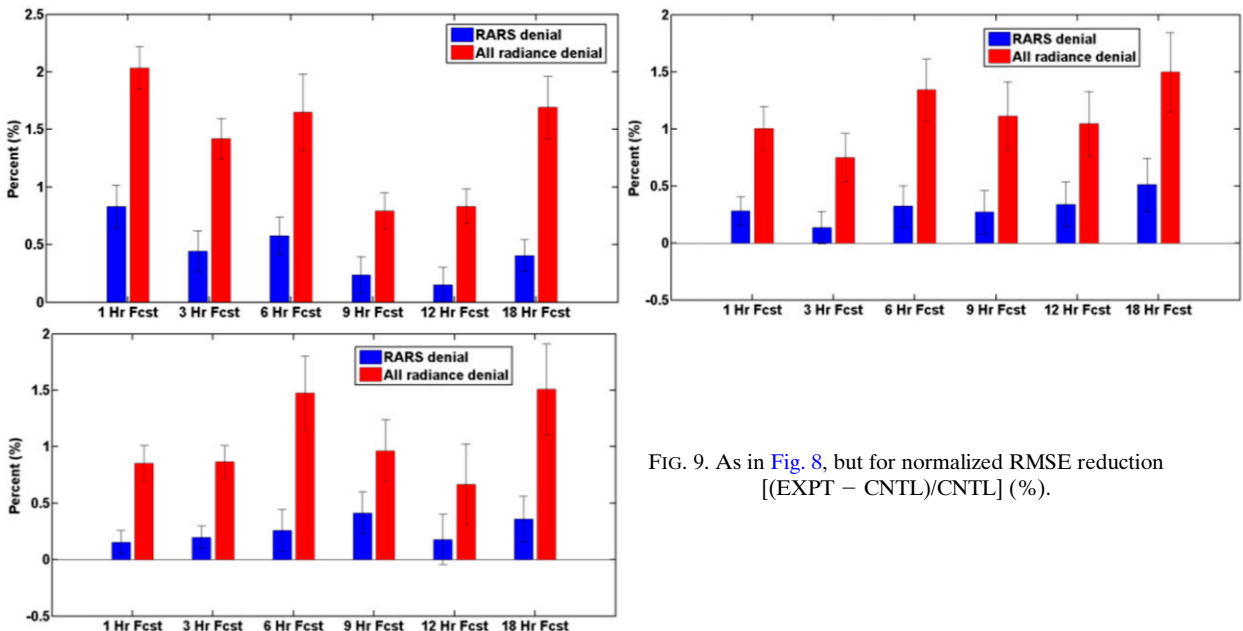


FIG. 9. As in Fig. 8, but for normalized RMSE reduction $[(EXPT - CNTL)/CNTL]$ (%).

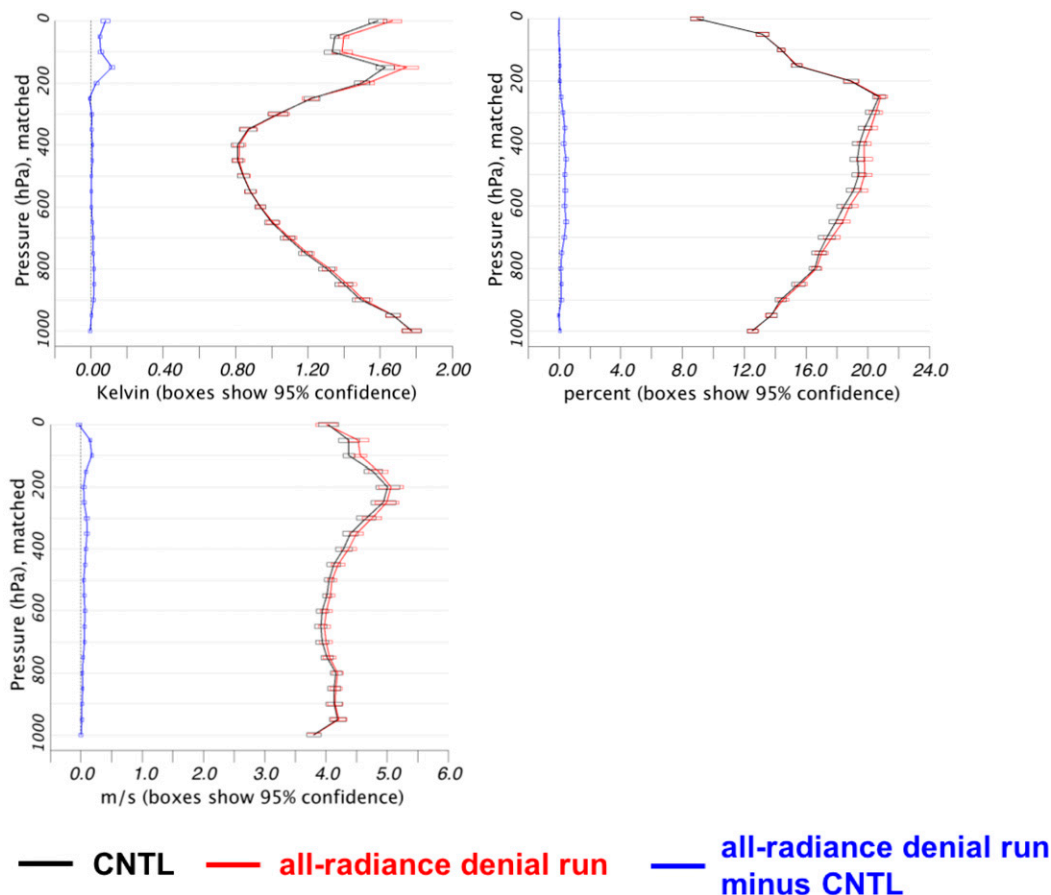


FIG. 10. RMSEs for (top left) temperature (K), (top right) relative humidity (%), and (bottom left) vector wind magnitude (m s^{-1}) for the control run (black) and all-radiance denial run (red) 6-h forecasts against rawinsonde observations over the RAP domain at isobaric levels every 50 hPa for a 1-month period (May 2013). The difference (all radiance denial run minus control run) is plotted in blue.

First, we look at the impact from the RARS data and from the all-radiance data. Figures 8 and 9 show the unnormalized and normalized 1–18-h forecast RMSE reductions (against radiosonde data, 1000–100 hPa averaged) of the RARS data-denial (blue) and all-radiance data-denial (red) runs compared with the CNTL run, respectively. We note that since the 6- and 18-h forecasts are initialized at times that have the longest interval since the introduction of global GFS information, which occurs at the end of the each partial cycle (0900 and 2100 UTC; see B16, section 2 for more details), the strongest data impact should be anticipated for these forecasts. It can be seen that radiance data have a very consistent small positive impact for all variables (temperature, relative humidity, and wind) and for all forecast lead times (1–18 h) with confidence at the 95% level. For temperature, the normalized impact is from 0.7% to 1.6% (1- and 18-h forecasts have the biggest impact, nearly 0.01- and 0.025-K RMS error reductions, respectively); for relative humidity, the

normalized impact is from 0.7% to 1.1% (6- and 18-h forecasts have the biggest impact, nearly 0.25% and 0.3% RMS error reductions, respectively); and for wind, the normalized impact is from 1.0% to 1.6% (6- and 18-h forecasts have the biggest impact, nearly 0.06 and 0.07 m s^{-1} RMS error reductions, respectively). The real-time RARS data alone also have positive impacts, with averaged normalized impacts of 0.3%–0.9% for temperature and 0.2%–0.3% for relative humidity and wind. Depending on the variables and forecast hours, it is noted that use of the RARS data contributes about 10%–35% of the data impact from the all-radiance dataset. It is also expected that other future low-data-latency direct-readout/broadcast data or/and low-latency geostationary data could contribute significantly if used within RAP. Radiance data from geostationary satellites with low data latency will be favorable for hourly updating model systems.

Figure 10 shows the 6-h forecast RMS profile errors from the all-radiance data-denial experiment compared

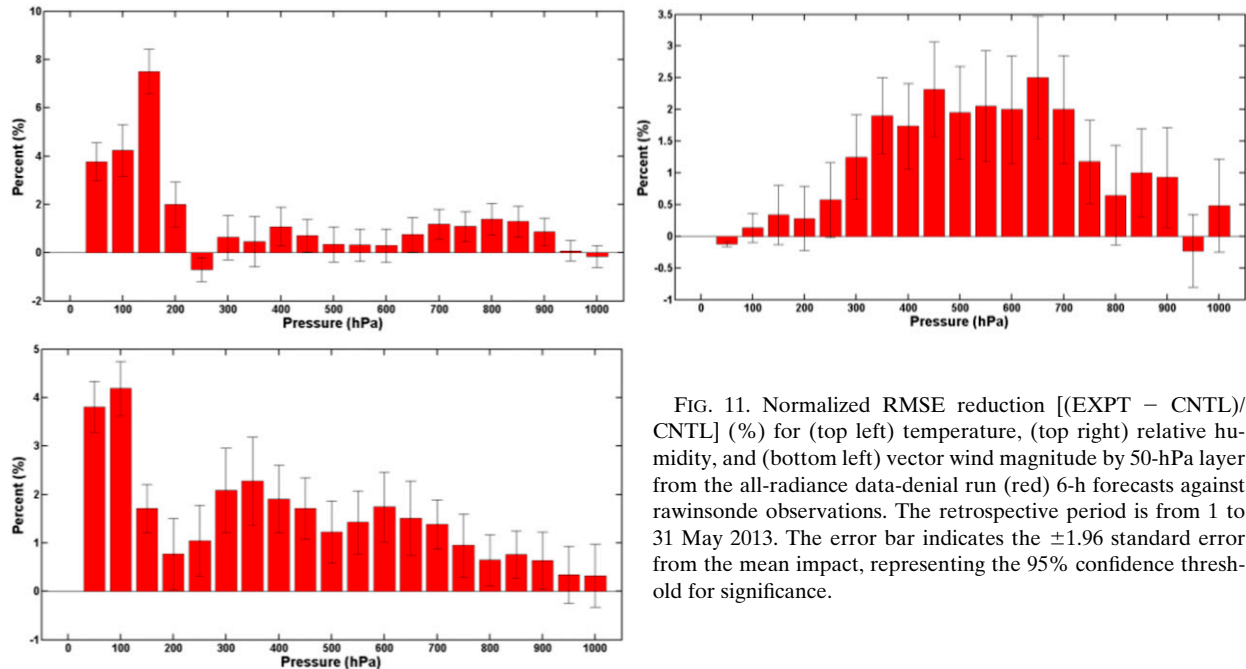


FIG. 11. Normalized RMSE reduction $[(\text{EXPT} - \text{CNTL}) / \text{CNTL}]$ (%) for (top left) temperature, (top right) relative humidity, and (bottom left) vector wind magnitude by 50-hPa layer from the all-radiance data-denial run (red) 6-h forecasts against rawinsonde observations. The retrospective period is from 1 to 31 May 2013. The error bar indicates the ± 1.96 standard error from the mean impact, representing the 95% confidence threshold for significance.

with the control run. It is noted that, for temperature, the largest positive impact (blue line, RMSE difference) is in the upper levels (above 200 hPa); for relative humidity, the largest impact from the radiances came from the middle levels (400–700 hPa); and for wind, the largest impact was above 400 hPa. Figure 11 shows the 6-h forecast normalized RMSE reduction against radiosonde data at each vertical level (50-hPa interval) from the all-radiance data-denial experiment compared with the control run. It can be seen that for temperature, the largest normalized impact (nearly 7%) is at 150 hPa; for relative humidity, the largest impact (more than 2%) is at 600 hPa; and for wind, the largest impact (more than 3%) is at 350 hPa. For a few vertical levels, there is very small forecast degradation. We also examined the all-radiance data impact on precipitation forecasts. The results mostly are neutral (not shown).

Next, we examine the forecast lead-time evolution of the all-radiance data impact from different atmospheric layers (surface and boundary, 1000–800 hPa; middle troposphere, 800–400 hPa; and from upper troposphere to lower stratosphere, 400–100 hPa). Figure 12 shows the normalized RMS error reduction (against radiosonde data) for these three layers from including the all-radiance data. It can be seen that for temperature (Fig. 12, top left), the largest normalized impact came from the 400–100-hPa layer with the biggest normalized impact being more than 2% at some forecast times. For relative humidity (Fig. 12, top right), the largest impact systematically came from the

800–400-hPa layer with a normalized impact of more than 1.5%. For wind (Fig. 12, bottom left), the biggest impact came from the 400–100-hPa layer with the biggest normalized impact of more than 2.5%. Also, as shown in Fig. 10, radiance data are expected to have the largest impact in the upper levels above 200 hPa for temperature and wind since RAP conventional data are usually sparse in this upper atmosphere.

To calibrate the radiance data impact in RAP, two additional data-denial (for aircraft and radiosondes) experiments were conducted. Figure 13 illustrates the normalized RMSE reduction (100–1000-hPa mean) from the all-radiance data-denial run (red), radiosonde data-denial run (blue), and aircraft data-denial run (green). Similar to results from James and Benjamin (2017), aircraft data have the largest impact (14% for temperature, more than 2% for relative humidity, and 8% for wind) among these three datasets. The impact from the radiance data and radiosonde data is relatively small compared with the impact from aircraft data, especially for temperature and wind. The radiance data impact is comparable with (sometimes superior to) the impact from the radiosonde data.

5. Summary and future work

The impact from real-time satellite radiance data within a NOAA hourly updating regional model system has been assessed and reported from 1-month retrospective runs. Adaptations were first made to better

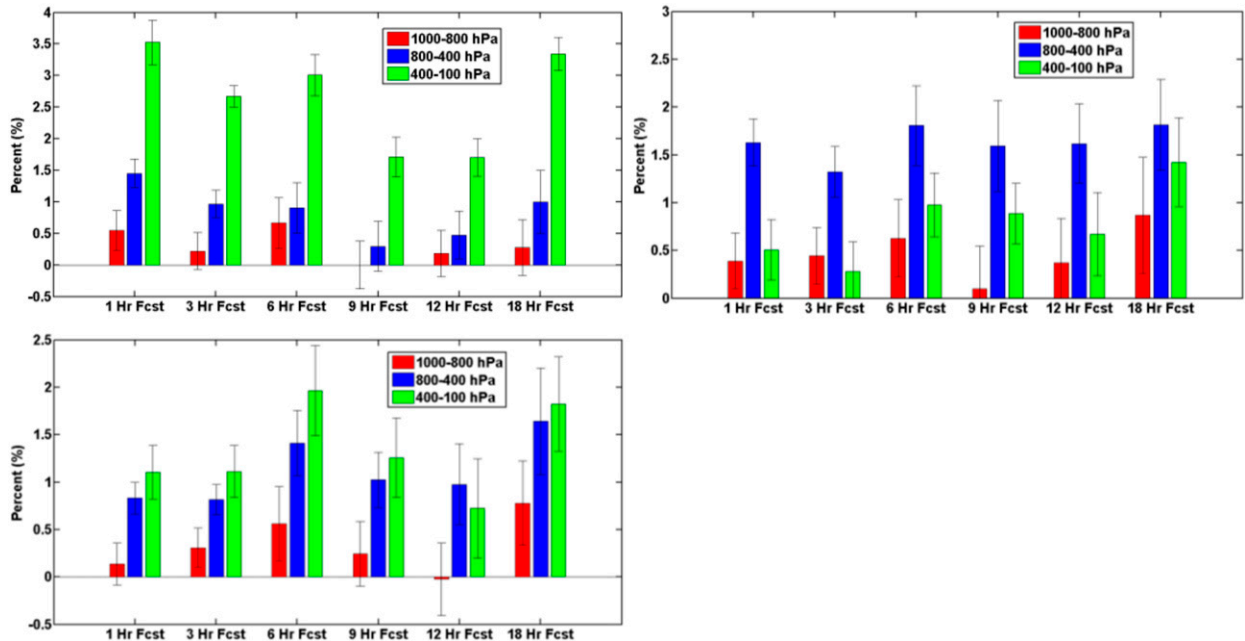


FIG. 12. Normalized RMSE reduction $[(\text{EXPT} - \text{CNTL})/\text{CNTL}]$ (%) for (top left) temperature, (top right) relative humidity, and (bottom left) vector wind magnitude for the 1000–800-hPa layer (red), the 800–400-hPa layer (blue), and the 400–100-hPa layer (green), from the all-radiance data-denial run 1–18-h forecasts against rawinsonde observations. Statistics are computed over the RAP domain. The retrospective period is from 1 to 31 May 2013. The error bar indicates the ± 1.96 standard error from the mean impact, representing the 95% confidence threshold for significance.

assimilate radiance data in the RAP model, including the use of real-time RARS direct-readout data, with the application of a new enhanced bias correction scheme within GSI, and appropriate channel selection. This configuration was applied to the operational RAP system, version 3, implemented at NCEP in August 2016.

A series of data-denial experiments was performed to assess the forecast impact from radiance data, as well as that from other conventional datasets (aircraft and rawinsonde). Short-range (1–18 h) forecast verification against radiosonde observations showed an overall positive impact with 95% significance when radiance data were assimilated. For the full atmospheric layer (1000–100-hPa layer), a consistent positive impact from radiance assimilation with significance was found for temperature, relative humidity and wind for all forecast hours with the largest normalized impact of 1.6% for temperature, 1.1% for relative humidity, and 1.6% for wind. The RARS data provide improved real-time data coverage for the RAP model, through lower latency, and are able to provide a substantial portion of the total radiance data impact for RAP with its tight data cutoff limits. Verification results also showed that radiance data have the largest impact for temperature in the 400–100-hPa layer (up to 3% reduction in RMSE), for relative humidity in the 800–400-hPa layer (more than 1.5%), and for wind in the 400–100-hPa layer (more than 2.5%).

Aircraft and radiosonde data-denial experiments were also conducted to evaluate the relative impact comparison of other conventional datasets with satellite radiance data. Radiosonde verification results showed that the radiance data impact is much smaller than the aircraft data, but it is often comparable with that from radiosonde data. One possible reason for the small improvement from radiance data in this study may be the absence of higher spectral infrared data. AIRS data assimilation within RAP is documented in Lin et al. (2017, manuscript submitted to *Wea. Forecasting*), and we are currently testing the assimilation of other high spectral infrared data [e.g., Cross-Track Infrared Sounder (CrIS) and Infrared Atmospheric Sounding Interferometer (IASI)] for the coming RAP version 4 implementation.

Satellite radiance data have been shown to have small but consistent positive impacts with significance for the hourly updated RAP model system. Reduced data latency now available through RARS direct readout was essential for this result. We plan to incorporate new satellite datasets [including the Joint Polar Satellite System (JPSS; Goldberg et al. 2013) and Geostationary Operational Environmental Satellite-R series (GOES-R, now *GOES-16*; Schmit et al. 2005, 2017)] through future direct readout and direct broadcast [e.g., Direct Broadcast Network for Near Real-Time Relay of Low Earth Orbit Satellite Data (DBNet)] into RAP or other hourly updated models in the future.

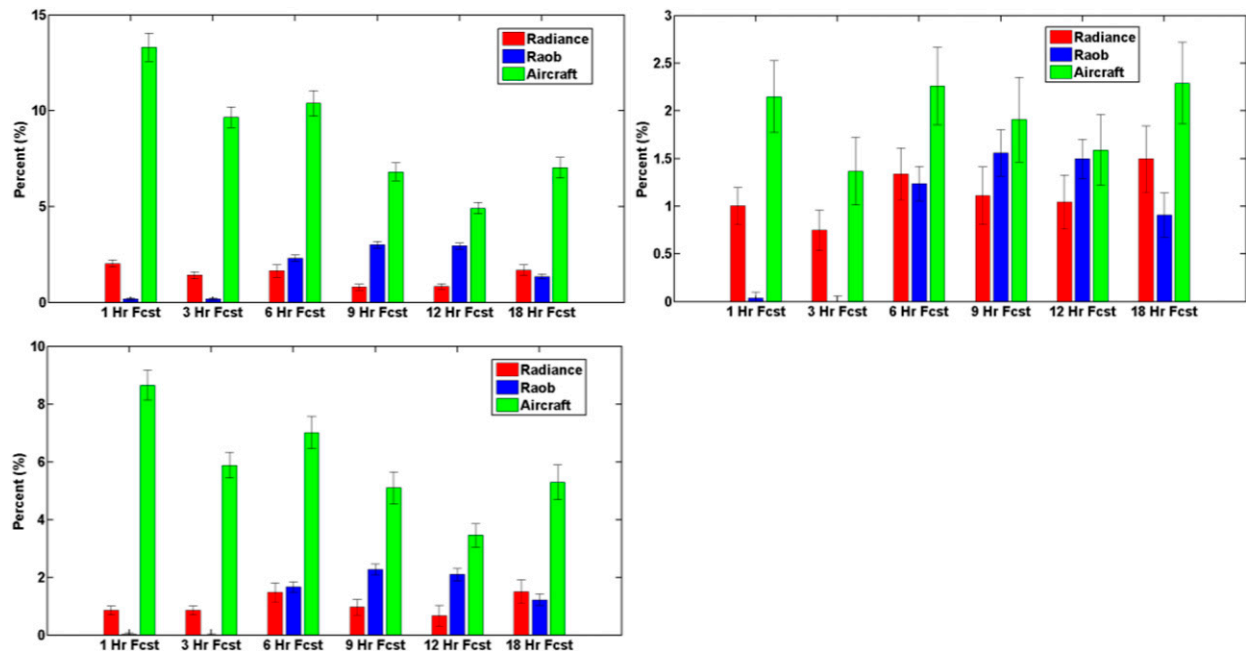


FIG. 13. Normalized RMSE reduction $[(\text{EXPT} - \text{CNTL})/\text{CNTL}]$ (%) for (top left) temperature, (top right) relative humidity, and (bottom left) vector wind magnitude from the all-radiance data-denial run (red), radiosonde data-denial run (blue), and aircraft data-denial run (green) 1–18-h forecasts against rawinsonde observations. Statistics are computed for the 1000–100-hPa layer over the RAP domain. The retrospective period is from 1 to 31 May 2013. The error bar indicates the ± 1.96 standard error from the mean impact, representing the 95% confidence threshold for significance.

Acknowledgments. This work was supported by NOAA Award NA14OAR4320125. The views, opinions, and findings contained in this report are those of the authors and should not be construed as an official National Oceanic and Atmospheric Administration or U.S. government position, policy, or decision. The authors thank Dr. John M. Brown of ESRL/GSD and three anonymous reviewers for thoughtful and very helpful reviews of this manuscript.

REFERENCES

- Andersson, E., J. Pailleux, J.-N. Thépaut, J. R. Eyre, A. P. McNally, G. A. Kelly, and P. Courtier, 1994: Use of cloud-cleared radiances in three/four-dimensional variational data assimilation. *Quart. J. Roy. Meteor. Soc.*, **120**, 627–653, doi:10.1002/qj.49712051707.
- Aumann, H. H., and Coauthors, 2003: AIRS/AMSU/HSB on the *Aqua* mission: Design, science objectives, data products, and processing systems. *IEEE Trans. Geosci. Remote Sens.*, **41**, 253–264, doi:10.1109/TGRS.2002.808356.
- Benjamin, S. G., and Coauthors, 2004a: An hourly assimilation/forecast cycle: The RUC. *Mon. Wea. Rev.*, **132**, 495–518, doi:10.1175/1520-0493(2004)132<0495:AHACTR>2.0.CO;2.
- , B. E. Schwartz, E. J. Zozke, and S. E. Koch, 2004b: The value of wind profiler data in U.S. weather forecasting. *Bull. Amer. Meteor. Soc.*, **85**, 1871–1886, doi:10.1175/BAMS-85-12-1871.
- , B. D. Jamison, W. R. Moninger, S. R. Sahn, B. Schwartz, and T. W. Schlatter, 2010: Relative short-range forecast impact from aircraft, profiler, radiosonde, VAD, GPS-PW, METAR, and mesonet observations via the RUC hourly assimilation cycle. *Mon. Wea. Rev.*, **138**, 1319–1343, doi:10.1175/2009MWR3097.1.
- , and Coauthors, 2016: A North American hourly assimilation and model forecast cycle: The Rapid Refresh. *Mon. Wea. Rev.*, **144**, 1669–1694, doi:10.1175/MWR-D-15-0242.1.
- Boukabara, S., K. Garrett, and V. Kumar, 2016: Potential gaps in the satellite observing system coverage: Assessment of impact on NOAA’s numerical weather prediction overall skills. *Mon. Wea. Rev.*, **144**, 2547–2563, doi:10.1175/MWR-D-16-0013.1.
- Dee, D. P., 2005: Bias and data assimilation. *Quart. J. Roy. Meteor. Soc.*, **131**, 3323–3343, doi:10.1256/qj.05.137.
- Derber, J. C., and W.-S. Wu, 1998: The use of TOVS cloud-cleared radiances in the NCEP SSI analysis system. *Mon. Wea. Rev.*, **126**, 2287–2299, doi:10.1175/1520-0493(1998)126<2287:TUOTCC>2.0.CO;2.
- Goldberg, M. D., H. Kilcoyne, H. Cikanek, and A. Mehta, 2013: Joint Polar Satellite System: The United States next generation civilian polar-orbiting environmental satellite system. *J. Geophys. Res.*, **118**, 13 463–13 475, doi:10.1002/2013JD020389.
- Han, Y., P. Van Delst, Q. Liu, F. Weng, B. Yan, R. Treadon, and J. Derber, 2006: JCSDA Community Radiative Transfer Model (CRTM) version 1. NOAA Tech. Rep. NESDIS 122, 31 pp. [Available online at http://www.emc.ncep.noaa.gov/research/JointOSSEs/Manuals/CRTM_v1_NOAAtechReport.pdf.]
- James, E. P., and S. G. Benjamin, 2017: Observation system experiments with the hourly updating Rapid Refresh model using GSI hybrid ensemble–variational data assimilation. *Mon. Wea. Rev.*, doi:10.1175/MWR-D-16-0398.1, in press.

- Jung, J. A., T. H. Zapotocny, J. F. Le Marshall, and R. E. Treadon, 2008: A two-season impact study on NOAA polar-orbiting satellites in the NCEP Global Data Assimilation System. *Wea. Forecasting*, **23**, 854–877, doi:10.1175/2008WAF2007065.1.
- Kazumori, M., 2014: Satellite radiance assimilation in the JMA operational mesoscale 4DVAR system. *Mon. Wea. Rev.*, **142**, 1361–1381, doi:10.1175/MWR-D-13-00135.1.
- Kleist, D. T., D. F. Parrish, J. C. Derber, R. Treadon, W.-S. Wu, and S. Lord, 2009: Introduction of the GSI into the NCEP Global Data Assimilation System. *Wea. Forecasting*, **24**, 1691–1705, doi:10.1175/2009WAF2222201.1.
- Lord, S., G. Gayno, and F. Zhang, 2016: Analysis of an observing system experiment for the Joint Polar Satellite System. *Bull. Amer. Meteor. Soc.*, **97**, 1409–1425, doi:10.1175/BAMS-D-14-00207.1.
- McNally, A. P., 2012: Observing system experiments to assess the impact of possible future degradation of the Global Satellite Observing Network. ECMWF Tech. Memo. 672, 20 pp. [Available online at www.ecmwf.int/sites/default/files/elibrary/2012/11085-observing-system-experiments-assess-impact-possible-future-degradation-global-satellite.pdf.]
- , J. C. Derber, W. Wu, and B. B. Katz, 2000: The use of TOVS level-1b radiances in the NCEP SSI analysis system. *Quart. J. Roy. Meteor. Soc.*, **126**, 689–724, doi:10.1002/qj.49712656315.
- , P. D. Watts, J. A. Smith, R. Engelen, G. A. Kelly, J. N. Thépaut, and M. Matricardi, 2006: The assimilation of AIRS radiance data at ECMWF. *Quart. J. Roy. Meteor. Soc.*, **132**, 935–957, doi:10.1256/qj.04.171.
- Moninger, W. R., S. G. Benjamin, B. D. Jamison, T. W. Schlatter, T. L. Smith, and E. J. Szoke, 2010: Evaluation of regional aircraft observations using TAMDAR. *Wea. Forecasting*, **25**, 627–645, doi:10.1175/2009WAF2222321.1.
- Schmit, T. J., M. M. Gunshor, W. P. Menzel, J. J. Gurka, J. Li, and A. S. Bachmeier, 2005: Introducing the next-generation Advanced Baseline Imager on GOES-R. *Bull. Amer. Meteor. Soc.*, **86**, 1079–1096, doi:10.1175/BAMS-86-8-1079.
- , P. Griffith, M. M. Gunshor, J. M. Daniels, S. J. Goodman, and W. J. Lebar, 2017: A closer look at the ABI on the GOES-R series. *Bull. Amer. Meteor. Soc.*, **98**, 681–698, doi:10.1175/BAMS-D-15-00230.1.
- Skamarock, W. C., and Coauthors, 2008: A description of the Advanced Research WRF version 3. NCAR Tech. Note NCAR/TN-475+STR, 113 pp., doi:10.5065/D68S4MVH.
- Smith, T. L., S. G. Benjamin, J. M. Brown, S. Weygandt, T. Smirnova, and B. Schwartz, 2008: Convection forecasts from the hourly updated, 3-km High Resolution Rapid Refresh (HRRR) model. *24th Conf. on Severe Local Storms*, Savannah, GA, Amer. Meteor. Soc., 11.1. [Available online at https://ams.confex.com/ams/24SLS/techprogram/paper_142055.htm.]
- Weng, F. Z., 2007: Advances in radiative transfer modeling in support of satellite data assimilation. *J. Atmos. Sci.*, **64**, 3799–3807, doi:10.1175/2007JAS2112.1.
- WMO, 2009: Final report of the WMO RARS Implementation Group and IGDDS Implementation Group Joint 3rd Meeting. WMO Final Rep., 37 pp. [Available online at http://www.wmo.int/pages/prog/sat/documents/RARS-IGDDS-IG-3_Final-Report.pdf.]
- Wu, W.-S., R. J. Purser, and D. F. Parrish, 2002: Three-dimensional variational analysis with spatially inhomogeneous covariances. *Mon. Wea. Rev.*, **130**, 2905–2916, doi:10.1175/1520-0493(2002)130<2905:TDVAWS>2.0.CO;2.
- Zhu, Y., J. Derber, A. Collard, D. Dee, R. Treadon, G. Gayno, and J. A. Jung, 2014: Enhanced radiance bias correction in the National Centers for Environmental Prediction's Gridpoint Statistical Interpolation data assimilation system. *Quart. J. Roy. Meteor. Soc.*, **140**, 1479–1492, doi:10.1002/qj.2233.